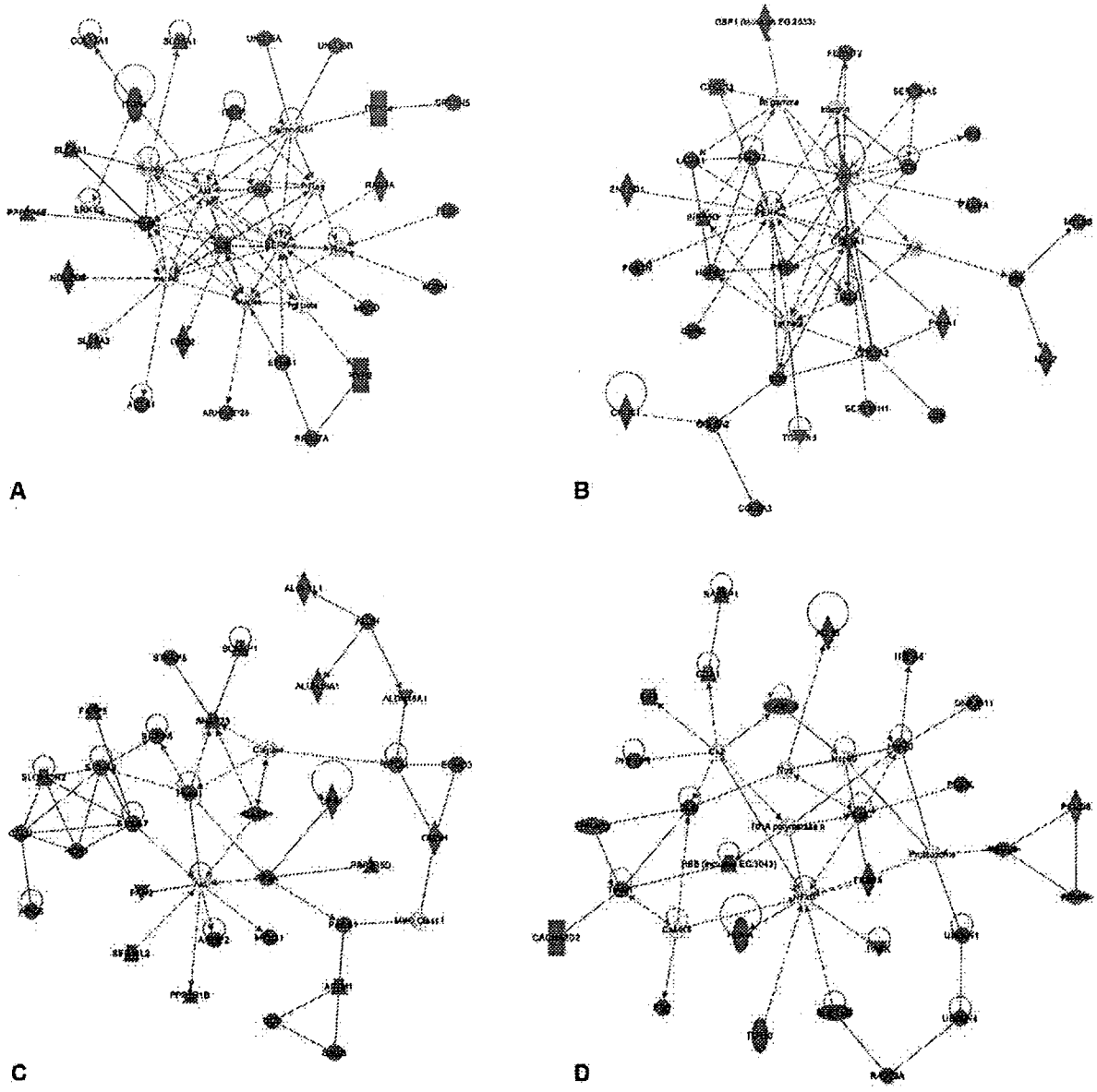

Figure 3 The molecular network of the AP, CAP, and CP proteome suggested by IPA. The list of Entrez Gene IDs of the MS lesion–specific proteome was uploaded onto the 'Core Analysis' tool of Ingenuity pathway analysis (IPA). Molecular networks most relevant to the AP (A), CAP (B and C), or CP (D) proteome are shown. Red nodes represent the molecules included in the gene list (Supplementary Tables 1–3). The molecular network (A) is constructed by 35 nodes, including ACTA1, AGRN, Akt, ARHGAP26, Calmodulin, CHD2, CHGA, COL17A1, EFNB1, ERK, ERK1/2, FGD1, HGF, insulin, ITGB4, ITSN1, MADD, Mapk, NDUFB9, Pkc(s), PP2A, PPP2R5E, RAB1A, Rac, Ras, RPS27A, RYR2, SLC2A3, SLC6A1, SLC8A1, SPTBN5, TGF-β, TRPC4, UNC13A, and UNC13B. The network (B) is constructed by 35 nodes, including BGN, CHI3L1, CNN2, COL1A1, COL1A2, COL6A2, COL6A3, CXCL11, ENTPD1, ERK, FBLN2, FERMT2, FN1, GBP1, HSPG2, IFN-γ, INPP5D, Integrin, LAMA1, LUM, Mlc, MYL7, MYL6B, NES, P4HA1, Pak, PARVA, POSTN, PRELP, SERPINA5, SERPINH1, TGF-β, TGFBR3, THBS1, and VTN. The network (C) is constructed by 35 nodes, including Akt, ALDH, ALDH16A1, ALDH18A1, ALDH1L1, AP1M1, APCS, ARFIP2, Calpain, CALU, CAST, DCD, FABP5, MHC Class I, MYH11, OGDH, PACS1, Pkc(s), PKN2, PP2A, PPP1R1B, PPP2R5D, RCN1, S100A7, S100A8, S100A9, SACS, SCAMP1, SEC14L2, SLC9A3R2, SNAP23, STOM, STXBP5, SUMO3, and UPF1. The network (D) is constructed by 35 nodes, including ADH5, AIP, CACNA2D2, CaMKII, Ck2, DMD, DNAJB11, EIF5, FKBP5, GGA1, HBB, HLA-A, Hsp70, Hsp90, HSPA6, NFkB, Nos, PASK, PEX5L, POMC, PPFIBP1, Proteasome, PSD, PSMB3, PSMB5, PSMD6, RABEP1, RAD23A, RNA polymerase II, SQSTM1, THRAP3, TIAM1, TLR10, UBQLN1, and UBQLN4. The molecular relation is indicated by solid line (direct interaction), dash line (indirect interaction), with filled arrow (acts on), stop (inhibits), stop and filled arrow (inhibits and acts on), and open arrow (translocates to).

Downloaded from http://msj.sagepub.com by Jun-ichi Satoh on April 24, 2009

Table 5 The molecular pathway relevant to MS brain-lesion proteome suggested by Ingenuity pathway analysis (IPA) search

Stage	Rank	Functional category	The number of genes classified	*P*-value
AP	1	Calcium signaling	7	2,53E-03
	2	Oxidative phosphorylation	4	2,69E-02
CAP	1	Calcium signaling	14	5,14E-04
	2	Hepatic fibrosis and hepatic stellate cell activation	11	1,53E-03
	3	Purine metabolism	16	3,05E-03
	4	Actin cytoskeleton signaling	13	5,77E-03
	5	Oxidative phosphorylation	9	1,12E-02
CP	1	Biosynthesis of steroids	4	7,37E-04
	2	Actin cytoskeleton signaling	8	8,00E-03
	3	Ubiquinone biosynthesis	4	9,54E-03
	4	Axonal guidance signaling	11	1,37E-02
	5	Integrin signaling	7	2,19E-02

The list of Entrez Gene IDs of MS brain-lesion proteome was uploaded onto the 'Core Analysis' tool of IPA. The canonical pathways relevant to the proteome data are shown with the number of genes classified and *P*-value.
Abbreviations: AP, acute plaques; CAP, chronic active plaques; and CP, chronic plaques.

the ECM and integrin signaling pathway to CAP and CP was further verified by molecular network analysis using PANTHER, KeyMolnet, and IPA followed by statistical evaluation. These *in silico* observations agree well with *in-vivo* studies, showing remarkable upregulation of diverse ECM constituents in MS brain lesions, where cytokine/chemokine-activated microglia, astrocytes, and infiltrating macrophages release a large amount of proteolytic enzymes bound to ECM molecules, which mediate myelin breakdown [17,18]. Glial scars in chronic lesions of MS include certain ECM proteins that contribute to the failure of regeneration of damaged axons and remyelination of preserved axons [17,18].

In active demyelinating lesions of MS, the expression of vitronectin is greatly enhanced in blood vessel walls, as well as in demyelinated axons and hypertrophic astrocytes at the edge of demyelination [19]. The levels of CD51, a vitronectin receptor, are elevated in the serum of relapsing-remitting MS patients [20]. Vitronectin promotes migration of reactive astrocytes expressing αvβ8 integrin [21]. In active demyelinating lesions of MS, fibronectin is accumulated in the brain parenchyma and is deposited abundantly in blood vessel walls and perivascular infiltrates [22]. Fibronectin facilitates migration of immune cells, promotes proliferation of astrocytes, and inhibits differentiation of oligodendrocyte progenitors [23]. In MS lesions, both vitronectin and fibronectin are derived mainly form plasma protein components passing across the disrupted blood–brain barrier and partly from the local synthesis by endothelial cells, macrophages, astrocytes, and infiltrating immune cells. Vitronectin and fibronectin activate microglia and upregulate MMP-9 production [24]. Thrombospondin produced by reactive astrocytes facilitates macrophage-mediated phagocytosis of apoptotic cells and possible uptake of degraded myelin via the ECM receptors CD36 and αvβ3 integrin [25]. Large-scale sequencing of MS plaque cDNA libraries showed that osteopontin (SPP1), a proinflammatory component of ECM, is one of the most abundant transcripts [26]. The clinical severity of EAE is attenuated in SPP1-deficient mice [26]. The expression of osteopontin is enhanced in astrocytes in active demyelinating lesions of MS [27]. The plasma osteopontin levels are elevated in active relapsing-remitting MS patients [28]. All of these observations support the concept that the selective blockade of the interaction between ECM and integrins in brain lesions *in situ* would be a target candidate for therapeutic intervention in MS.

Because focal adhesion kinase (FAK) is a central mediator of the integrin signaling pathway (see Figure 1), one possible choice is the use of an inhibitor for ECM-induced autophosphorylation of FAK [29]. TAE226, a FAK inhibitor, suppresses tumor cell invasion *in vivo* [29]. Another option for integrin signaling inhibitors is disintegrins, a group of small disulfide-rich peptides containing the arginine–glycine–aspartic acid sequence that mediates the selective binding to integrins [30]. Liposomal delivery of contortrostatin, a snake venome disintegrin, shows a tumor-suppressive anti-angiogenic activity [30]. However, a complete blockade of general function of integrins has a risk for inducing serious side effects [31]. Even in the context of the selective blockade, treatment with a humanized monoclonal antibody against VLA4, α4β1 integrin (natalizumab) reduced relapses 66% in clinical trials of MS but also activated the lethal infection of JC virus in some patients [32].

Downloaded from http://msj.sagepub.com by Jun-ichi Satoh on April 24, 2009

Acknowledgments

This work was supported by grants to J-IS from Research on Psychiatric and Neurological Diseases and Mental Health, the Ministry of Health, Labour and Welfare of Japan (H17-020), Research on Health Sciences Focusing on Drug Innovation, the Japan Health Sciences Foundation (KH21101), the Grant-in-Aid for Scientific Research, the Ministry of Education, Culture, Sports, Science and Technology, Japan (MEXT) (B18300118), the High-Tech Research Center Project, MEXT (S0801043) and from the Nakatomi Foundation.

References

1. Lassmann, H, Brück, W, Lucchinetti, CF. The immunopathology of multiple sclerosis: an overview. *Brain Pathol* 2007; **17**: 210–218.
2. Kieseier, BC, Wiendl, H, Hemmer, B, Hartung, HP. Treatment and treatment trials in multiple sclerosis. *Curr Opin Neurol* 2007; **20**: 286–293.
3. Kingsmore, SF, Lindquist, IE, Mudge, J, Gessler, DD, Beavis, WD. Genome-wide association studies: progress and potential for drug discovery and development. *Nat Rev Drug Discov* 2008; **7**: 221–230.
4. Steinman, L, Zamvil, S. Transcriptional analysis of targets in multiple sclerosis. *Nat Rev Immunol* 2003; **3**: 483–492.
5. Quintana, FJ, Farez, MF, Weiner, HL. Systems biology approaches for the study of multiple sclerosis. *J Cell Mol Med* 2008; doi 10.1111/j.1582-4934.2008.00375.x.
6. Lock, C, Hermans, G, Pedotti, R, *et al.* Gene-microarray analysis of multiple sclerosis lesions yields new targets validated in autoimmune encephalomyelitis. *Nat Med* 2002; **8**: 500–508.
7. Satoh, J, Nakanishi, M, Koike, F, *et al.* Microarray analysis identifies an aberrant expression of apoptosis and DNA damage-regulatory genes in multiple sclerosis. *Neurobiol Dis* 2005; **18**: 537–550.
8. Han, MH, Hwang, SI, Roy, DB, *et al.* Proteomic analysis of active multiple sclerosis lesions reveals therapeutic targets. *Nature* 2008; **451**: 1076–1081.
9. Ganter, B, Giroux, CN. Emerging applications of network and pathway analysis in drug discovery and development. *Curr Opin Drug Discov Devel* 2008; **11**: 86–94.
10. Viswanathan, GA, Seto, J, Patil, S, Nudelman, G, Sealfon, SC. Getting started in biological pathway construction and analysis. *PLoS Comput Biol* 2008; **4**: e16.
11. Albert, R, Jeong, H, Barabasi, AL. Error and attack tolerance of complex networks. *Nature* 2000; **406**: 378–382.
12. Kanehisa, M, Araki, M, Goto, S, *et al.* KEGG for linking genomes to life and the environment. *Nucleic Acids Res* 2008; **36**: D480–D484.
13. Mi, H, Guo, N, Kejariwal, A, Thomas, PD. PANTHER version 6: protein sequence and function evolution data with expanded representation of biological pathways. *Nucleic Acids Res* 2007; **35**: D247–D252.
14. Palacios, R, Goni, J, Martinez-Forero, I, *et al.* A network analysis of the human T-cell activation gene network identifies JAGGED1 as a therapeutic target for autoimmune diseases. *PLoS ONE* 2007; **2**: e1222.
15. Sato, H, Ishida, S, Toda, K, *et al.* New approaches to mechanism analysis for drug discovery using DNA microarray data combined with KeyMolnet. *Curr Drug Discov Technol* 2005; **2**: 89–98.
16. Luo, BH, Carman, CV, Springer, TA. Structural basis of integrin regulation and signaling. *Annu Rev Immunol* 2007; **25**: 619–647.
17. Sobel, RA. The extracellular matrix in multiple sclerosis lesions. *J Neuropathol Exp Neurol* 1998; **57**: 205–217.
18. van Horssen, J, Dijkstra, CD, de Vries, HE. The extracellular matrix in multiple sclerosis pathology. *J Neurochem* 2007; **103**: 1293–1301.
19. Sobel, RA, Chen, M, Maeda, A, Hinojoza, JR. Vitronectin and integrin vitronectin receptor localization in multiple sclerosis lesions. *J Neuropathol Exp Neurol* 1995; **54**: 202–213.
20. Minagar, A, Jy, W, Jimenez, JJ, *et al.* Elevated plasma endothelial microparticles in multiple sclerosis. *Neurology* 2001; **56**: 1319–1324.
21. Milner, R, Huang, X, Wu, J, *et al.* Distinct roles for astrocyte αvβ5 and αvβ8 integrins in adhesion and migration. *J Cell Sci* 1999; **112**: 4271–4279.
22. Sobel, RA, Mitchell, ME. Fibronectin in multiple sclerosis lesions. *Am J Pathol* 1989; **135**: 161–168.
23. Sisková, Z, Baron, W, de Vries, H, Hoekstra, D. Fibronectin impedes "myelin" sheet-directed flow in oligodendrocytes: a role for a beta 1 integrin-mediated PKC signaling pathway in vesicular trafficking. *Mol Cell Neurosci* 2006; **33**: 150–159.
24. Milner, R, Crocker, SJ, Hung, S, Wang, X, Frausto, RF, del Zoppo, GJ. Fibronectin- and vitronectin-induced microglial activation and matrix metalloproteinase-9 expression is mediated by integrins $\alpha_5\beta_1$ and $\alpha_v\beta_5$. *J Immunol* 2007; **178**: 8158–8167.
25. Ren, Y, Savill, J. Proinflammatory cytokines potentiate thrombospondin-mediated phagocytosis of neutrophils undergoing apoptosis. *J Immunol* 1995; **154**: 2366–2374.
26. Chabas, D, Baranzini, SE, Mitchell, D, *et al.* The influence of the proinflammatory cytokine, osteopontin, on autoimmune demyelinating disease. *Science* 2001; **294**: 1731–1735.
27. Sinclair, C, Kirk, J, Herron, B, Fitzgerald, U, McQuaid, S. Absence of aquaporin-4 expression in lesions of neuromyelitis optica but increased expression in multiple sclerosis lesions and normal-appearing white matter. *Acta Neuropathol* 2007; **113**: 187–194.
28. Vogt, MH, Lopatinskaya, L, Smits, M, Polman, CH, Nagelkerken, L. Elevated osteopontin levels in active relapsing-remitting multiple sclerosis. *Ann Neurol* 2003; **53**: 819–822.
29. Liu, TJ, LaFortune, T, Honda, T, *et al.* Inhibition of both focal adhesion kinase and insulin-like growth factor-I receptor kinase suppresses glioma proliferation *in vitro* and *in vivo*. *Mol Cancer Ther* 2007; **6**: 1357–1367.
30. Swenson, S, Costa, F, Minea, R, *et al.* Intravenous liposomal delivery of the snake venom disintegrin contortrostatin limits breast cancer progression. *Mol Cancer Ther* 2004; **3**: 499–511.
31. Cantor, JM, Ginsberg, MH, Rose, DM. Integrin-associated proteins as potential therapeutic targets. *Immunol Rev* 2008; **223**: 236–251.
32. Steinman, L. Blocking adhesion molecules as therapy for multiple sclerosis: natalizumab. *Nat Rev Drug Discov* 2005; **4**: 510–518.

Downloaded from http://msj.sagepub.com by Jun-ichi Satoh on April 24, 2009

Disease Markers 27 (2009) 239–252
DOI 10.3233/DMA-2009-0670
IOS Press

Molecular network analysis suggests aberrant CREB-mediated gene regulation in the Alzheimer disease hippocampus

Jun-ichi Satoh[a,*], Hiroko Tabunoki[a] and Kunimasa Arima[b]
[a]*Department of Bioinformatics and Molecular Neuropathology, Meiji Pharmaceutical University, 2-522-1 Noshio, Kiyose, Tokyo 204-8588, Japan*
[b]*Department of Psychiatry, National Center Hospital, National Center of Neurology and Psychiatry, 4-1-1 Ogawahigashi, Kodaira, Tokyo 187-8551, Japan*

Abstract. The pathogenesis of Alzheimer disease (AD) involves the complex interaction between genetic and environmental factors affecting multiple cellular pathways. Recent advances in systems biology provide a system-level understanding of AD by elucidating the genome-wide molecular interactions. By using KeyMolnet, a bioinformatics tool for analyzing molecular interactions on the curated knowledgebase, we characterized molecular network of 2,883 all stages of AD-related genes (ADGs) and 559 incipient AD-related genes (IADGs) identified by global gene expression profiling of the hippocampal CA1 region of AD brains in terms of significant clinical and pathological correlations (Blalock et al., Proc Natl Acad Sci USA 101: 2173-2178, 2004). By the common upstream search, KeyMolnet identified cAMP-response element-binding protein (CREB) as the principal transcription factor exhibiting the most significant relevance to molecular networks of both ADGs and IADGs. The CREB-regulated transcriptional network included upregulated and downregulated sets of ADGs and IADGs, suggesting an involvement of generalized deregulation of the CREB signaling pathway in the pathophysiology of AD, beginning at the early stage of the disease. To verify the *in silico* observations *in vivo*, we conducted immunohistochemical studies of 11 AD and 13 age-matched control brains by using anti-phoshorylated CREB (pCREB) antibody. An abnormal accumulation of pCREB imunoreactivity was identified in granules of granulovacuolar degeneration (GVD) in the hippocampal neurons of AD brains. These observations suggest that aberrant CREB-mediated gene regulation serves as a molecular biomarker of AD-related pathological processes, and support the hypothesis that sequestration of pCREB in GVD granules is in part responsible for deregulation of CREB-mediated gene expression in AD hippocampus.

Keywords: Alzheimer disease, CREB, granulovacuolar degeneration, keymolnet, molecular network, systems biology

1. Introduction

Alzheimer disease (AD) is the most common cause of dementia worldwide, affecting the elderly population, characterized by the hallmark pathology of amyloid-β (Aβ) deposition and neurofibrillary tangle (NFT) formation in the brain. The complex interaction between genetic and environmental factors affecting multiple cellular pathways plays a role in the pathogenesis of AD [1]. The completion of the Human Genome Project in 2003 allows us to systematically characterize the comprehensive disease-associated profiles of the whole human genome. It promotes us to identify disease-specific and stage-specific molecular signatures and biomarkers for diagnosis and prediction of prognosis, and druggable targets for therapy [2]. Actually, global transcriptome analysis of AD brains identified a battery of genes aberrantly regulated in AD, whose role has not been previously

*Corresponding author: Prof. Dr. Jun-ichi Satoh, Department of Bioinformatics and Molecular Neuropathology, Meiji Pharmaceutical University, 2-522-1 Noshio, Kiyose, Tokyo 204-8588, Japan. Tel./Fax: +81 42 495 8678; E-mail: satoj@my-pharm.ac.jp.

ISSN 0278-0240/09/$17.00 © 2009 – IOS Press and the authors. All rights reserved

predicted in its pathogenesis. They include reduced expression of kinases/phosphatases, cytoskeletal proteins, synaptic proteins, and neurotransmitter receptors in NFT-bearing CA1 neurons [3], downregulaton of neurotrophic factors and upregulation of proapoptotic molecules in the hippocampal CA1 region [4], disturbed sphingolipid metabolism in various brain regions during progression of AD [5], and overexpression of the AMPA receptor GluR2 subunit in synaptosomes of prefrontal cortex [6]. However, in global expression analysis, the important biological implications are often left behind to be characterized, because the huge amount of high-density microarray data is highly complex. Furthermore, cardinal observations obtained from *in silico* data analysis should be validated by independent wet lab experiments.

Recent advances in systems biology enable us to illustrate a cell-wide map of the complex molecular interactions with aid of the literature-based knowledgebase of molecular pathways [7,8]. In the scale-free molecular network, targeted disruption of several critical components, on which the biologically important molecular connections concentrate, could disturb the whole cellular function by destabilizing the network [9]. Thus, molecular network analysis goes beyond gene-by-gene analysis to shed light on a system-level understanding of molecular relationships among individual genes and networks.

The present study is designed to conduct molecular network analysis of a published microarray dataset of Blalock et al. [10]. It contains genome-wide expression profiling of hippocampal CA1 tissues derived from 22 AD patients with well-defined clinical and pathological stages. They identified 3,413 all stages of AD-related genes (ADGs) and 609 incipient AD-related genes (IADGs), and characterized overrepresented genes by using a bioinformatics tool named Expression Analysis Systematic Explorer (EASE). They found upregulation of tumor suppressors, oligodendrocyte growth factors, and protein kinase A (PKA) modulators, along with downregulation of protein folding/metabolism/transport machinery molecules in incipient AD (IAD) [10]. Recently, a different study followed up analysis of this dataset by weighted gene coexpression network analysis (WGCNA) that calculates a matrix containing all pairwise Pearson correlations between whole microarray probe sets across all subjects in an unsupervised manner. They identified AD-related coexpression modules that play key roles in synaptic transmission, extracellular transport, mitochondrial and metabolic functions, and myelination [11]. However, all of these studies did not clarify the common upstream transcription factors governing molecular networks, closely associated with deregulated gene expression in AD brains. By using KeyMolnet, a bioinformatics tool for analyzing molecular interactions on the curated knowledgebase [12], we characterized the most relevant molecular network of AD brain transcriptome, composed of the genes coordinately regulated by putative common upstream transcription factors.

2. Materials and methods

2.1. The dataset

We performed molecular network analysis of ADGs and IADGs, derived from a dataset of Blalock et al. [10]. It contains gene expression profiling of frozen tissues of the CA1 hippocampus, performed by analyzing with the Affymetrix Human Genome HG-U133A chip that contains 22,215 transcripts. The complete dataset is available from Gene Expression Omnibus (GEO) database (GSE1297). RNA was isolated from the samples of 31 age-matched individuals, composed of nine control subjects, seven patients with incipient AD (IAD), eight with moderate AD, and seven with severe AD [10]. The dataset was normalized following the Microarray Analysis Suite 5.0 (MAS5) algorithm. The clinical stage of AD was defined by the Mini-Mental State Examination (MMSE) score, i.e. control (MMSE $>$ 25), incipient AD (MMSE 20–26), moderate AD (MMSE 14–19), and severe AD (MMSE $<$ 14). The neurofibrillary tangle (NFT) burden was determined in each brain sample, which always showed an inverse relationship with the MMSE score. The statistical correlation between the expression levels of individual genes and the MMSE and NFT scores was evaluated by Pearson's correlation tests and ANOVA. With respect to overall correlations across 31 subjects, the study identified 3,413 ADGs, composed of 1,977 upregulated and 1,436 downregulated genes in all stages of AD patients versus control subjects. The study also identified 609 IADGs, composed of 431 upregulated and 178 downregulated genes in IAD patients versus control subjects.

2.2. Gene ID conversion

We converted Affymetrix probe IDs into the corresponding National Center for Biotechnology Information (NCBI) Entrez Gene IDs by using the

Database for Annotation, Visualization and Integrated Discovery (DAVID) 2008 Gene ID conversion tool (david.abcc.ncifcrf.gov) [13]. Then, we excluded a set of non-annotated genes, overlapping genes, and those listed concurrently in both upregulated and downregulated classes.

2.3. Molecular network analysis

KeyMolnet is a comprehensive knowledgebase, originally developed by the Institute of Medicinal Molecular Design (IMMD), Tokyo, Japan [12]. It covers virtually all the relationships heretofore reported among human genes, molecules, diseases, pathways and drugs, whose information is manually collected, carefully curated, and regularly updated by expert biologists. The database is categorized into the core contents collected from selected review articles with the highest reliability, or the secondary contents extracted from abstracts of PubMed database and Human Protein Reference database (HPRD). By importing microarray data, such as the list of Entrez Gene ID and fold changes of individual probes, KeyMolnet automatically provides corresponding molecules as a node on networks.

The common upstream search is a mode of network analysis that extracts the most relevant molecular network composed of the genes coordinately regulated by putative common upstream transcription factors. The generated network was compared side by side with 403 human canonical pathways of the KeyMolnet library. To reduce the potential bias toward the selection of major pathways, all well-established biological pathways covering both major and minor classes were collected by extensive search of valid review articles with journal impact factors greater than 10. Further information on the canonical pathways of KeyMolnet is available from IMMD upon request (www.immd.co.jp/en/keymolnet/index.html). The algorithm counting the number of overlapping molecular relations between the extracted network and the canonical pathway makes it possible to identify the canonical pathway showing the most significant contribution to the extracted network. It is constructed by modification of the algorithm developed for GO::TermFinder [14]. The significance in the similarity between the extracted network and the canonical pathway is scored following the formula, where O = the number of overlapping molecular relations between the extracted network and the canonical pathway, V = the number of molecular relations located in the extracted network, C = the number of molecular relations located in the canonical pathway, T = the number of total molecular relations composed of approximately 110,000 sets, and the X = the sigma variable that defines coincidence.

$$\text{Score} = -\log_2(\text{Score}(p))$$

$$\text{Score}(p) = \sum_{x=O}^{Min(C,V)} f(x)$$

$$f(x) = {}_C C_x \cdot {}_{T-C} C_{V-x} / {}_T C_V$$

2.4. Immunohistochemistry

The autopsied brain samples were provided by Research Resource Network (RRN), Japan. Written informed consent was obtained form all the cases. The Ethics Committee of National Center of Neurology and Psychiatry approved the present study. The study population consists of 11 AD patients composed of five men and six women with the mean age of 71 ± 9 years, and 13 other neurological disease (termed as non-AD) patients composed of six men and seven women with the mean age of 69 ± 9 years. The non-AD cases include three patients with Parkinson disease (PD), two with multiple system atrophy (MSA), four with amyotrophic lateral sclerosis (ALS), and four with myotonic dystrophy. The average of brain weight was 1,038 ± 163 gram in AD cases and 1,195 ± 182 gram in non-AD cases. Brain tissues of the hippocampus and the motor cortex were fixed with 4% paraformaldehyde (PFA), embedded in paraffin, and processed for ten micron-thick serial sections. All AD cases were satisfied with the Consortium to Establish a Registry for Alzheimer's Disease (CERAD) criteria for diagnosis of definite AD [15]. They were categorized into the stage C of amyloid deposition and the stage VI of neurofibrillary degeneration, following the Braak's staging [16].

The immunohistochemistry protocol was described elsewhere [17]. In brief, after deparaffination, tissue sections were heated in 10 mM citrate sodium buffer, pH 6.0 by autoclave at 125°C for 30 sec in a temperature-controlled pressure chamber (Dako, Tokyo, Japan). They were incubated with 3% hydrogen peroxide-containing methanol to block the endogenous peroxidase activity, and with phosphate-buffered saline (PBS) containing 10% normal goat serum (NGS) at room temperature (RT) for 15 min to block non-specific staining. Then, tissue sections were stained at 4°C overnight with rabbit polyclonal anti-phoshorylated cAMP-response element-binding protein (pCREB) an-

tibody at a dilution of 1:1,000 (Y011052; Applied Biological Materials, Richmond, BC, Canada). This antibody was produced against a synthesized phosphopeptide spanning R-P-SP-Y-R, derived from the human CREB1 amino acid sequences surrounding the serine 133 residue (Ser-133), and purified by affinity-chromatography with an epitope-specific phosphopeptide. The specificity of the antibody was verified by western blot analysis of a human neuronal cell line exposed to forskolin in culture (not shown). After several washes, the tissue sections were incubated with horseradish peroxidase (HRP)-conjugated anti-rabbit antibody (Nichirei, Tokyo, Japan), and colorized with DAB substrate (Vector Laboratories, Burlingame, CA, USA), followed by a counterstain with hematoxylin. The adjacent sections were immunolabeled with mouse monoclonal anti-GFAP antibody (Nichirei). For negative controls, the step of incubation with primary antibodies was omitted.

3. Results

3.1. *Transcriptome dataset of Alzheimer disease hippocampus*

The dataset of Blalock et al. [10] contains genome-wide transcriptome of the hippocampus CA1 region, derived from nine control subjects, seven patients with incipient AD (IAD), eight with moderate AD, and seven with severe AD. They identified 3,413 all stages of AD-related genes (ADGs) and 609 IAD-related genes (IADGs) based on significant clinical and pathological correlations. We performed extensive curation of their data, and extracted 2,883 Entrez Gene IDs of ADGs, composed of 1,675 upregulated and 1,208 downregulated genes in all stages of AD patients versus control subjects (Supplementary Tables 1 and 2 online). We also identified 559 Entrez Gene IDs of IADGs, composed of 395 upregulated and 164 downregulated genes in IAD patients versus control subjects (Supplementary Tables 3 and 4 online).

3.2. *The molecular network analysis of ADGs and IADGs identified CREB as a central transcription factor*

First, we imported 2,883 Entrez Gene IDs of ADGs, along with the expression levels, into KeyMolnet (the version 4.9.9.616 of July 1, 2009). The common upstream search of the core contents generated a complex network composed of 508 fundamental nodes with 735 molecular relations, arranged with respect to subcellular location of the molecules by the editing function of KeyMolnet (Fig. 1). By statistical evaluation, the extracted network showed the most significant relationship with transcriptional regulation by CREB with the score of 229 and score (p) = 1.141E-069, where CREB is located as a common upstream transcription factor that has direct connections with 50 nodes, all of which are known CRE-responsive genes (Fig. 2 and Table 1). Unexpectedly, the CREB-regulated transcriptional network is comprised of not only 17 upregulated ADGs but also 26 downregulated ADGs. These results suggest not simply either overactivation or hypoactivation of CREB but an involvement of generalized deregulation of the CREB signaling pathway in the pathophysiology of AD. The second rank pathway was transcriptional regulation by nuclear factor kappa B (NF-κB) with the score of 158 and score (p) = 1.945E-048 (Supplementary Fig. 1 online), while the third rank was transcriptional regulation by vitamin D receptor (VDR) with the score of 140 and score (p) = 5.841E-042 (Supplementary Fig. 2 online).

Next, we imported 559 Entrez Gene IDs of IADGs and the expression levels into KeyMolnet. Subsequently, the common upstream search of the core contents generated a less complex network composed of 143 fundamental nodes with 190 molecular relations (Fig. 3). By statistical evaluation, the extracted network showed again the most significant relationship with transcriptional regulation by CREB with the score of 71 and score (p) = 3.325E-022, comprised of 5 upregulated and 5 downregulated IADGs (Fig. 4 and Table 1). These results suggest that functional impairment of CREB in the AD hippocampus is beginning at the early stage of the disease. The second rank pathway was transcriptional regulation by NF-κB or by glucocorticoid receptor (GR) with the identical score of 53 and score (p) = 1.163E-016 between both.

3.3. *Granulovacuolar degeneration in hippocampal neurons of AD brains expressed pCREB immunoreactivity*

It is well known that a wide range of extracellular stimuli activates CREB by inducing phosphorylation of Ser-133 on CREB, thereby it functions as a transcriptional activator [18,19]. Because the molecular network of both ADGs and IADGs reflects persistent impairment of CREB function in the AD hippocampus, we studied the expression of Ser-133-phosphorylated

Table 1
The list of 51 genes constructing the CREB-regulated transcriptional network in AD hippocampus

KeyMolnet symbol	Gene name	Upregulation or downregulation[a]	Involvement in IAD network	Swiss-Prot ID
14-3-3epsilon	14-3-3 protein epsilon	down		P62258
AChE	acetylcholinestrase	down		P22303
AhR	arylhydrocarbon receptor	km		P35869
BCKDH	branched-chain alpha-keto acid dehydrogenase	down		P09622, P11182, P12694, P21953
Bcl-2	B-cell lymphoma 2	up		P10415
BiP	78 kDa glucose-regulated protein	down	yes	P11021
BRCA1	breast cancer type 1 susceptibility protein	up		P38398
C/EBPb	CCAAT/enhancer binding protein beta	km	yes	P17676
CCK	cholecystokinin	down		P06307
CDK5	cyclin dependent kinase 5	down		Q00535
ChromograninA	chromogranin A	down		P10645
CPT	carnitine palmitoyl transferase	up	yes	P50416, Q92523, Q8TCG5, P23786
CREB	cAMP-response-element-binding-protein	km	yes	P16220
CRF	corticotropin-releasing factor	down	yes	P06850
cyclinA	cyclin A	down		P78396, P20248
cyto-c	cytochrome c	down		P99999
DIO2	type II iodothyronine deiodinase	down		Q92813
Egr1	early growth response protein 1	up		P18146
ENO2	neuron-specific enolase	down		P09104
FN1	fibronectin 1	down		P02751
GADD34	protein phosphatase 1, regulatory subunit 15A	up		O75807
GluR1	glutamate receptor 1	down		P42261
GR	glucocorticoid receptor	km	yes	P04150
GS	glutamine synthetase	down	yes	P15104
HO-1	heme oxygenase 1	up		P09601
ICAM-1	intercellular adhesion molecule 1	up		P05362
IGF1	insulin-like growth factor 1	down		P01343, P05019
IL-6	interleukin-6	up		P05231
JunD	transcription factor Jun-D	up	yes	P17535
LDH	L-lactate dehydrogenase	down		Q6ZMR3, Q9BYZ2, P00338, P07195, P07864
MITF	microphthalmia-associated transcription factor	up	yes	O75030
MnSOD	manganese superoxide dismutase	up		P04179
NF-L	neurofilament triplet L protein	down		P07196
NPY	neuropeptide Y	down		P01303
NR4A2	orphan nuclear receptor NR4A2	km		P43354
ODC	ornithine decarboxylase	up		P11926
PC	prohormone convertase	down		P29120, P16519, Q16549
PCB	pyruvate carboxylase	up	yes	P11498
PCNA	proliferating cell nuclear antigen	down		P12004
PER1	period circadian protein 1	up	yes	O15534
PER2	period circadian protein 2	up		O15055
Pit-1	pituitary-specific positive transcription factor 1	km	yes	P28069
PPT-A	preprotachykinin A	down	yes	P20366
proenkeph	proenkephalin	down		P01213, P01210
SGK	serum- and glucocorticoid-inducible kinase	up	yes	O00141, Q9HBY8, Q96BR1
SST	somatostatin	down	yes	P61278
STAT3	signal transducer and activator of transcription 3	km	yes	P40763
SynapsinI	synapsin-1	down		P17600
TGFb2	transforming growth factor beta 2	up		P61812
TyrAT	tyrosine aminotransferase	up		P17735
VIP	vasoactive intestinal peptide	down		P01282

Km represents additional nodes unlisted in the original set of 2,883 ADGs but automatically incorporated from KeyMolnet core contents following the network-searching algorithm.

CREB (pCREB) in 11 AD and 13 age-matched control brains by immunohistochemistry. The granular components of granulovacuolar degeneration (GVD), accumulated in the cytoplasm of hippocampal pyramidal neurons in both AD and non-AD brains, expressed strong immunoreactivity against pCREB (Fig. 5, panels a-d). However, the nuclei of hippocampal pyramidal neurons were devoid of pCREB immunoreac-

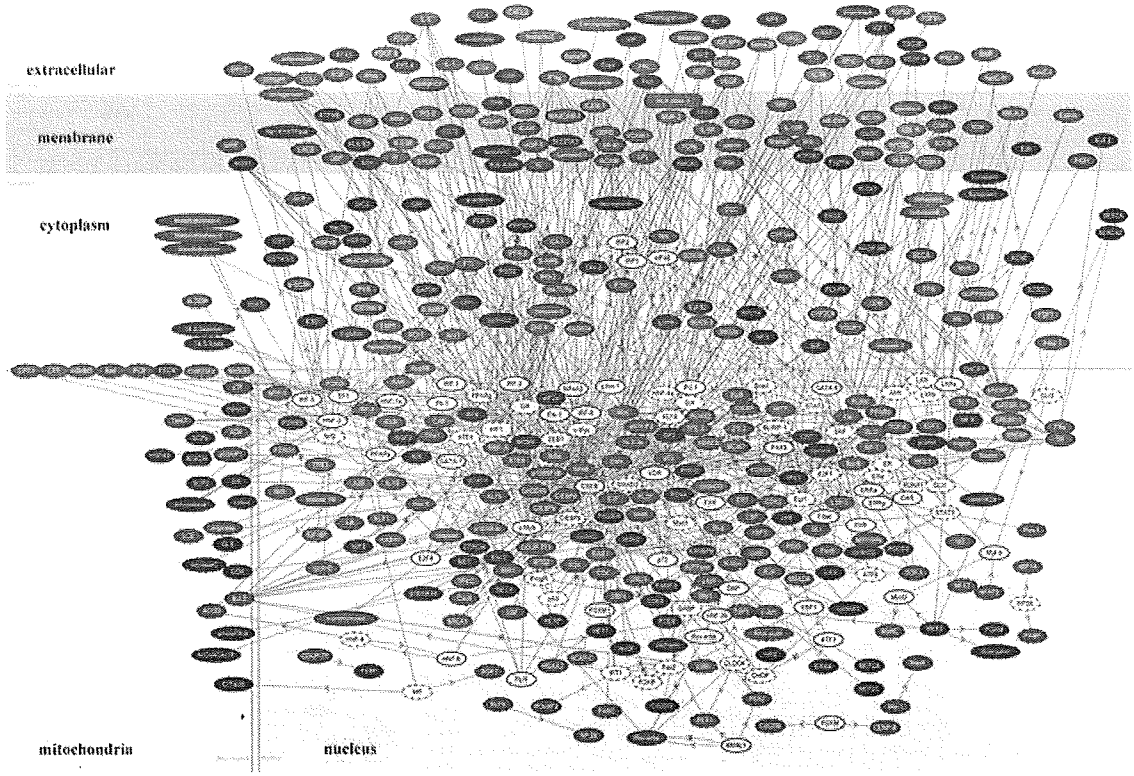

Fig. 1. Molecular network of all stages of AD-related genes (ADGs). The list of 2,883 Entrez Gene IDs corresponding to ADGs was imported into KeyMolnet. The common upstream search of the core contents generated a network composed of 508 fundamental nodes with 735 molecular relations, arranged with respect to subcellular location of the molecules. Red nodes represent upregulated genes, whereas blue nodes represent downregulated genes. White nodes exhibit additional nodes extracted automatically from the core contents incorporated in the network to establish molecular connections. The direction of molecular relation is indicated by red-colored dash line with arrow (transcriptional activation) or blue-colored dash line with arrow and stop (transcriptional repression).

tivity. In addition, the vacuolar component of GVD lacked pCREB immunoreactivity, while neuritic processes of hippocampal neurons expressed variable levels of pCREB immunoreactivity (Fig. 5, panel c). pCREB-immunoreactive GVD-bearing neurons were distributed chiefly in the CA1-CA3 sectors. Senile plaques and neurofibrillary tangles were completely devoid of pCREB immunolabeling. Although the number of pCREB-immunoreactive GVD-bearing neurons was varied among the cases, it was significantly greater in the hippocampus of AD compared with non-AD ($p = 0.00020$ by Mann-Whiteney's U test) (Fig. 6). pCREB-immunoreactive GVD-bearing neurons were occasionally found in the CA4 and subicular regions of AD brains, but barely detectable in the corresponding regions of non-AD brains. In both AD and non-AD brains, substantial numbers of neuronal axons distributed in the white matter of the motor cortex expressed intense pCREB immunoreactivity (Fig. 5, panel e). In both AD and non-AD brains, a subpopulation of reactive astrocytes and almost all ependymal cells expressed strong pCREB immunoreactivity, but it was located predominantly in their nuclei (Fig. 5, panel f). In both AD and non-AD brains, most neurons except for hippocampal pyramidal neurons did not express discernible pCREB immunoreactivity in their cell bodies and nuclei. Neither oligodendrocytes nor microglia expressed pCREB immunoreactivity in any cases examined.

4. Discussion

Since microarray analysis usually produces a large amount of gene expression data at one time, it is often difficult to find out the meaningful relationship be-

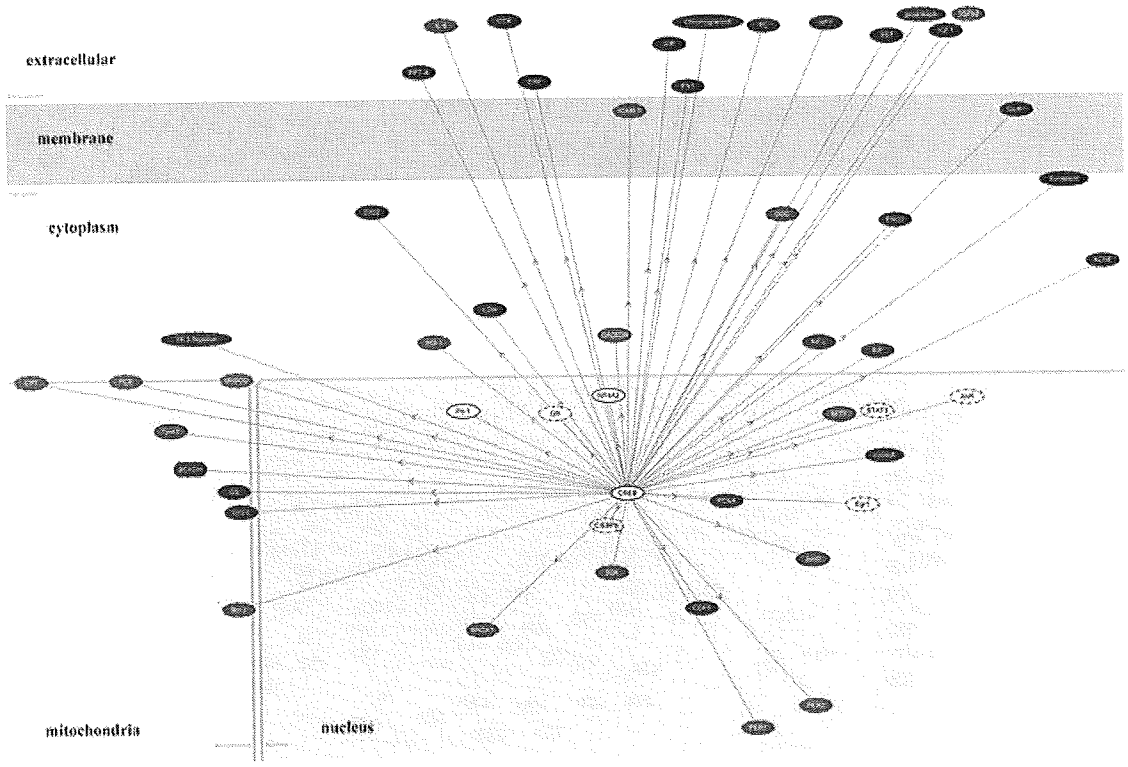

Fig. 2. The CREB-regulated transcriptional network of ADGs. The CREB-regulated transcriptional network extracted from the ADG network of Fig. 1 consists of a central node of CREB and 50 connecting nodes of CREB target genes listed in Table 1.

tween gene expression profile and biological implications from such a large quantity of available data. To overcome this difficulty, we have made a breakthrough to identify the molecular network most closely associated with microarray data by using a novel bioinformatics tool named KeyMolnet [12]. KeyMolnet includes the highly reliable information on a wide range of human proteins, small molecules, molecular relations, diseases, and drugs. All the contents are manually collected and carefully curated by experts from the literature and public databases. The application of KeyMolnet has an advantage that the user can easily merge microarray data with the comprehensive knowledgebase to characterize pathophysiologically meaningful networks from the high-throughput gene expression data [20,21]. In particular, the common upstream search is the most powerful approach to identify a battery of common transcription factors governing molecular networks closely associated with aberrant gene expression. By using KeyMolnet, we characterized the molecular network of 2,883 ADGs and 559 IADGs that show significant correlations with MMSE score and NFT burden in either all stages of AD or the early stage of AD [10]. We identified CREB as the central transcription factor that exhibits the most significant relevance to molecular networks of both ADGs and IADGs.

CREB is the prototype stimulus-inducible transcription factor binding as a dimer to a conserved cAMP-responsive element (CRE) of the target genes [18,19]. CREB is promptly activated in response to a wide range of extracellular stimuli, such as growth factors, peptide hormones, and neuronal activity, all of which activate various protein kinases such as PKA, mitogen-activated protein kinases (MAPKs), and Ca^{2+}/calmodulin-dependent protein kinases (CAMKs). They phosphorylate Ser-133 located in the KID domain of CREB. The phosphorylation of Ser-133 on CREB (pCREB) induces the recruitment of a transcriptional coactivator named CREB binding protein (CBP), thereby activates the expression of CRE-responsive genes. The CREB target genes play key roles in neuronal devel-

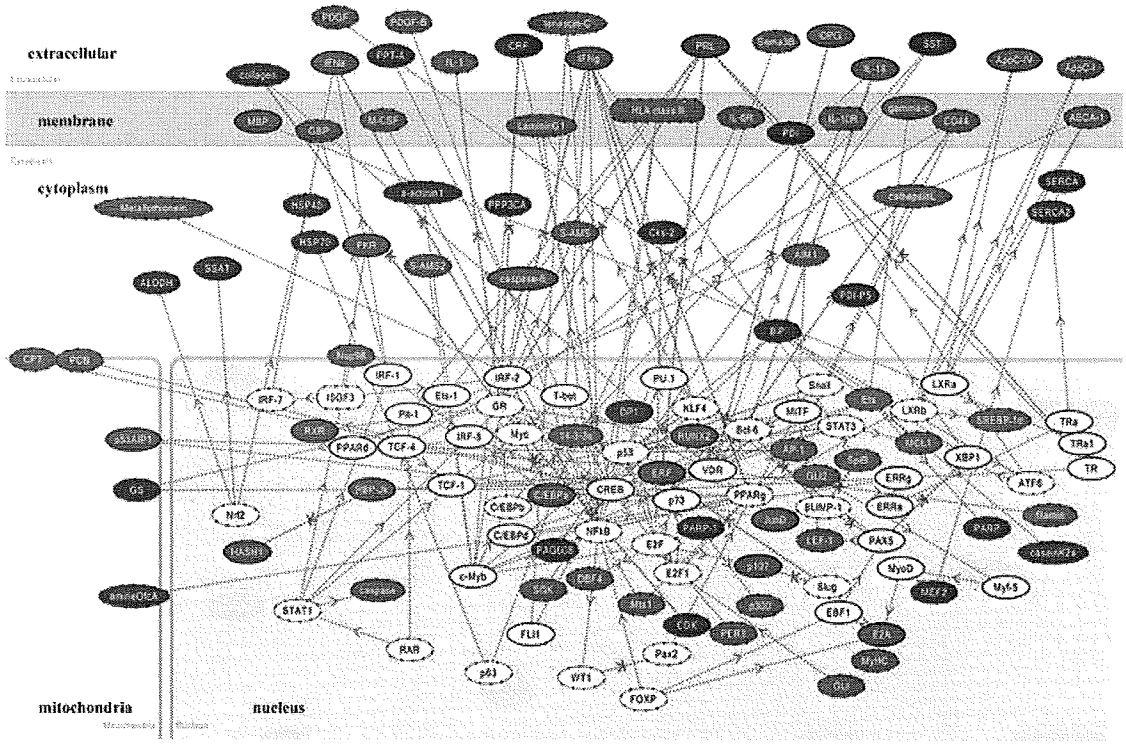

Fig. 3. Molecular network of incipient AD-related genes (IADGs). The list of 559 Entrez Gene IDs corresponding to IADGs was imported into KeyMolnet. The common upstream search of the core contents generated a network composed of 143 fundamental nodes with 190 molecular relations, arranged with respect to subcellular location of the molecules. Red nodes represent upregulated genes, whereas blue nodes represent downregulated genes. White nodes exhibit additional nodes extracted automatically from the core contents incorporated in the network to establish molecular connections. The direction of molecular relation is indicated by red-colored dash line with arrow (transcriptional activation) or blue-colored dash line with arrow and stop (transcriptional repression).

opment, synaptic plasticity, and neuroprotection in the central nervous system (CNS). Currently, we are able to search thousands of CREB target genes via the web-accessible database (natural.salk.edu/CREB) [22]. In the present study, the CREB-regulated transcriptional network consisted of both upregulated and downregulated sets of ADGs and IADGs. These observations suggest not simply either overactivation or hypoactivation of CREB but an involvement of generalized deregulation of the CREB signaling pathway in the pathophysiology of AD, emerging at the early stage of the disease.

To verify the *in silico* observations *in vivo*, we conducted immunohistochemical studies of 11 AD and 13 age-matched non-AD control brains by using anti-pCREB antibody. We identified aberrant pCREB immunoreactivity concentrated in granules of GVD in the hippocampus of both AD and non-AD brains, where the number of pCREB-immunoreactive GVD-bearing neurons was significantly greater in AD than non-AD cases. These results suggest that pCREB-immunoreactive GVD does not itself serve as an AD-specific diagnostic marker. However, these observations would support the hypothesis that sequestration of pCREB in GVD granules might be in part attributable to disturbed CREB-regulated gene expression in AD hippocampus.

Physiologically, CREB plays a pivotal role in the long-term memory formation in CA1 hippocampal neurons [23]. A previous study by western blot analysis showed that pCREB levels are reduced in AD brain tissues, although the cellular and subcellular location of pCREB was not characterized [24]. In a rat model, cortical impact injury induces a cognitive impairment, associated with reduced expression of CREB and target genes in the ipsilateral hippocampus [25]. A phosphodiesterase-4 inhibitor rolipram, by activating the cAMP/PKA/CREB signaling pathway, ameliorates deficits in long-term potential and cognitive function

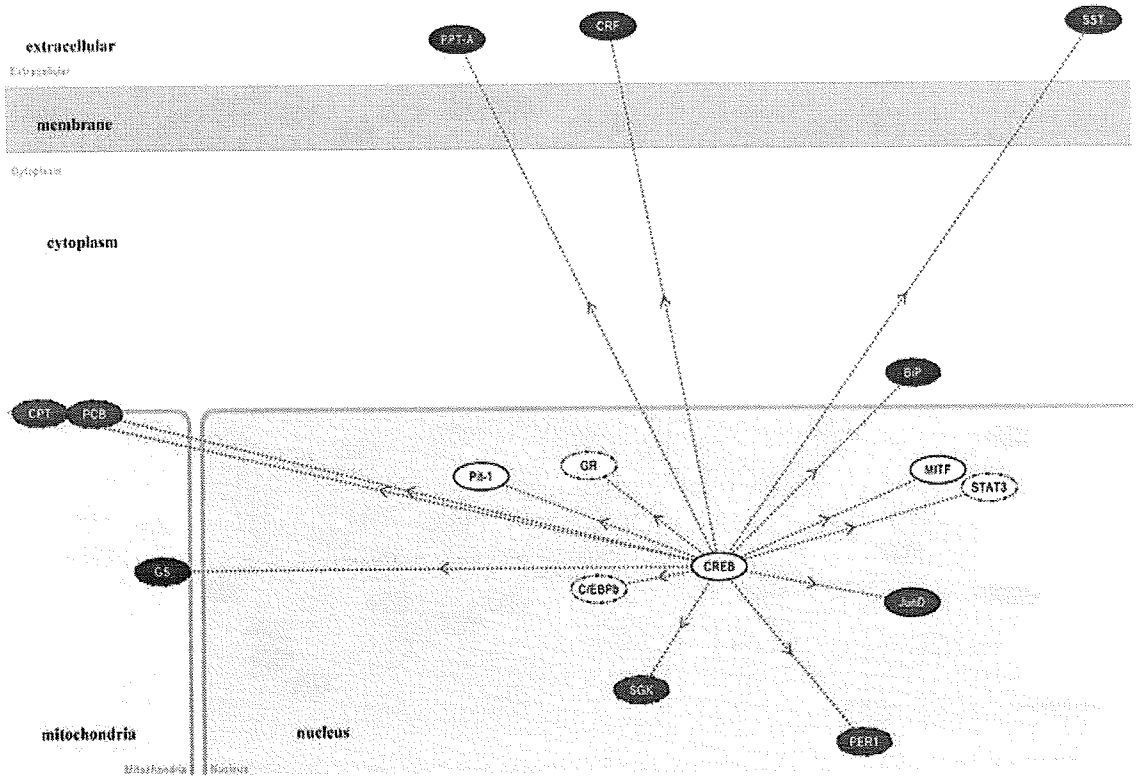

Fig. 4. The CREB-regulated transcriptional network of IADGs. The CREB-regulated transcriptional network extracted from the IADG network of Fig. 3 consists of a central node of CREB and 15 connecting nodes of CREB target genes listed in Table 1.

in a transgenic mouse model of AD [26]. Overactivation of calpain induces proteolysis of PKA subunits, resulting in inactivation of CREB in AD brains [27]. High levels of intracellular Aβ induce sustained hyperphosphorylation of CREB that blocks nuclear translocation of pCREB, resulting in inactivation of CREB-regulated gene expression [28]. The Aβ oligomers inactivate MAPKs, PKA, and cyclic GMP-dependent protein kinase essential for CREB activation in hippocampal neurons [29–31]. Long-term treatment with green tea catechin reduces the levels of Aβ oligomers, thereby restores the expression of CREB target genes, such as BDNF and PSD95, in the hippocampus [32]. All of these observations support a possible scenario that a defect in the CREB-mediated signaling pathway in hippocampal neurons causes cognitive disturbance during progression of AD. Therefore, CREB serves as a promising molecular target for treatment of dementia in AD [33].

The accumulation of misfolded cellular proteins within neurons, due to a defect in the clearance system, such as the ubiquitin-proteasome system (UPS) and the autophagic-lysosomal system, is a pathological hallmark of various neurodegenerative diseases [34]. Degradation of CREB involves nuclear export of CREB, modification by polyubiquitination, and processing for proteasomes, suggesting that UPS is a major system for CREB degradation under normal physiological conditions [35,36]. We identified an abnormal accumulation of pCREB in GVD granules of hippocampal neurons in AD brains. GVD is a pathological change characterized by electron-dense granules within double membrane-bound cytoplasmic vacuoles that highly resemble autophagosomes [37]. The emergence of GVD is confined to hippocampal pyramidal neurons of AD brains, and infrequently found in those of other neurodegenerative diseases. GVD is barely detectable in other brain regions. It plays a role in sequestration and degradation of unnecessary proteins and organelles in neurons exposed to aging-related stressful insults [37]. The active forms of caspase-3, glycogen synthase kinase-3β (GSK-3β), c-Jun N-terminal kinase

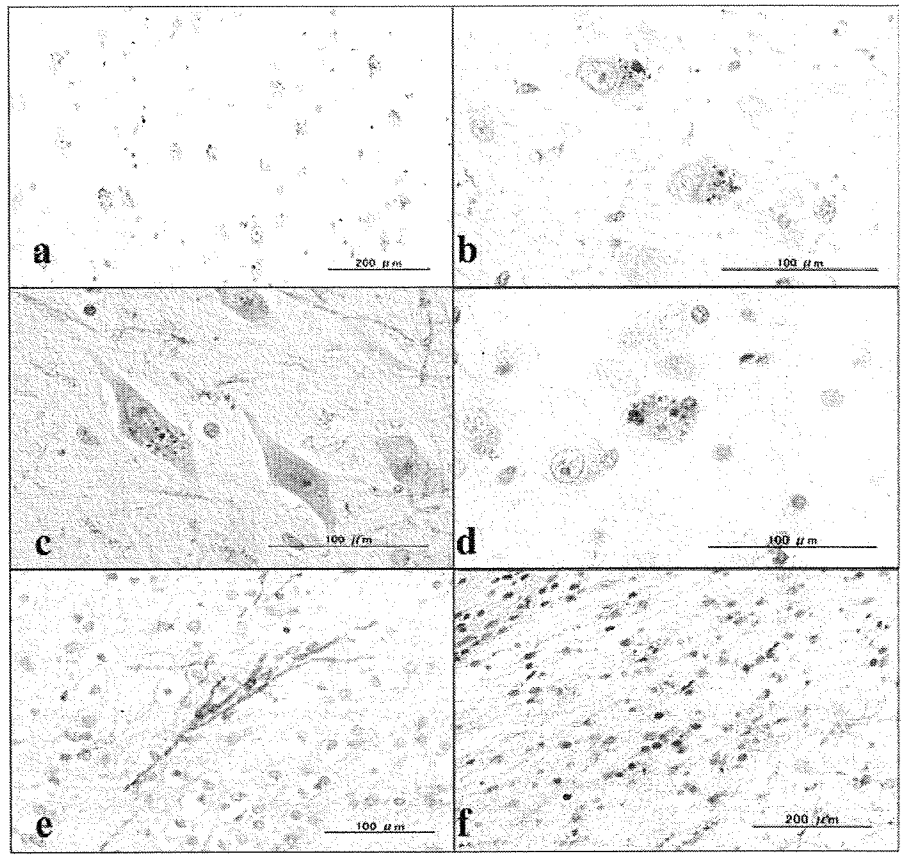

Fig. 5. pCREB immunoreactivity in AD and non-AD brains. The tissue sections of the hippocampus (HC) and the motor cortex (MC) of 11 AD patients and 13 other neurological disease (non-AD) patients were immunolabeled with an antibody against Ser-133-phosphorylated CREB (pCREB). (a) HC CA1 of a 59-year-old AD patient. The granular components of granulovacuolar degeneration (GVD) accumulated in the cytoplasm of pyramidal neurons exhibit strong pCREB immunoreactivity. (b) HC CA1 of a 68-year-old AD patient. The granular components of GVD accumulated in the cytoplasm of pyramidal neurons exhibit strong pCREB immunoreactivity. (c) HC CA3 of a 77 year-old AD patient. The vacuolar components of GVD are devoid of pCREB immunoreactivity. Neuritic processes of hippocampal neurons express variable levels of pCREB immunoreactivity. (d) HC CA1 of a 68 year-old myotonic dystrophy patient. The granular components of GVD accumulated in the cytoplasm of pyramidal neurons exhibit strong pCREB immunoreactivity. (e) MC of a 72-year-old AD patient. Substantial numbers of neuronal axons in the white matter of the motor cortex express strong pCREB immunoreactivity. (f) The periventricular white matter in the hippocampus of an 80 year-old AD patient. A subpopulation of reactive astrocytes express strong pCREB immunoreactivity located predominantly in their nuclei.

(JNK), c-Jun, pancreatic eIF2-alpha kinase (PERK), and TAR DNA-binding protein-43 (TDP-43), all of which are modified by phosphorylation, are found to be accumulated in GVD granules of hippocampal neurons in AD brains [38–43]. GVD granules also include cytoskeletal proteins, such as neurofilament, tubulin, and tau, along with ubiquitin [44,45]. At present, the precise implication of pCREB accumulation in GVD granules of hippocampal neurons in AD brains remains unknown. Importantly, degenerating neurons but not apparently healthy neurons in AD brains exhibit the profuse accumulation of autophagic vacuoles (AVs), owing to decreased clearance of AVs [46], suggesting an involvement of impaired autophagy function in formation of pCREB-accumulated GVD granules.

We found that neuronal axons, neuritic processes, and a subpopulation of reactive astrocytes also express pCREB immunoreactivity in both AD and non-AD brains. In a rat model of neuronal injury, reactive astrocytes express pCREB following intracerebroventricular injection of kinate [47]. In developing mouse DRG neurons, CREB protein is translated in response to NGF from the corresponding mRNA located in axons, and subsequently translocated to the cell body via a retro-

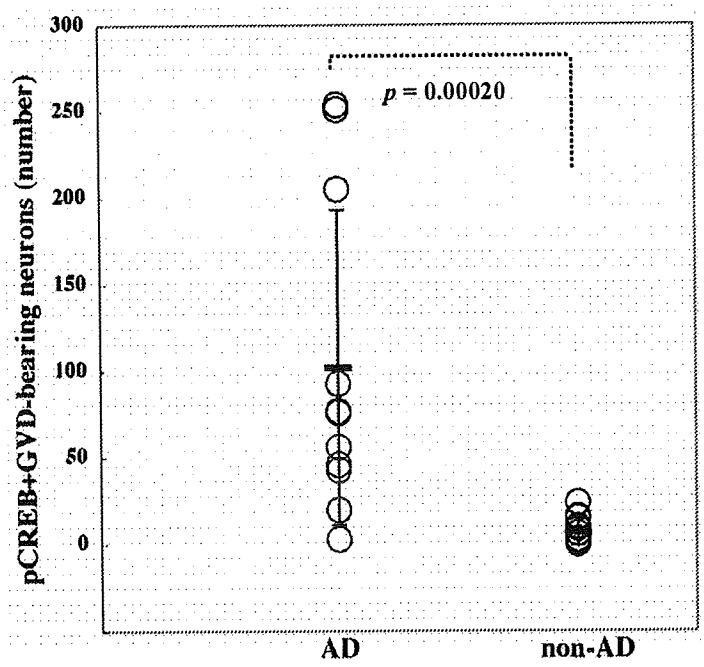

Fig. 6. The number of pCREB-immunoreactive GVD-bearing neurons in the hippocampus of AD and non-AD brains. The number of pCREB-immunoreactive GVD-bearing neurons was counted in the CA1, CA2, CA3 and CA4 sectors and the subiculum of the hippocampus, derived from 11 AD cases and 13 age and sex-matched other neurological disease (non-AD) cases. Non-AD cases include three patients with Parkinson disease (PD), two with multiple system atrophy (MSA), four with amyotrophic lateral sclerosis (ALS), and four with myotonic dystrophy. The total number in each case is plotted. The statistical difference in the numbers between AD and non-AD was evaluated by Mann-Whitney's U test.

grade axonal transport [48]. These observations would provide an explanation for glial or axonal location of CREB and pCREB.

We identified NF-κB-regulated gene expression as the second significant pathway in the molecular network of AGDs and IADGs (Supplementary Fig. 1 online). The NF-κB family, consisting of NF-κB1 (p50/p105), NF-κB2 (p52/p100), RelA (p65), RelB, and c-Rel, acts as a central regulator of innate and adaptive immune responses, cell proliferation, and apoptosis [49]. Under unstimulated conditions, NF-κB is sequestrated in the cytoplasm via non-covalent interaction with the inhibitor of NF-κB (IκB). Proinflammatory cytokines and stress-inducing agents activate specific IκB kinases that phosphorylate IκB proteins. Phosphorylated IκBs are ubiquitinated, and then processed for proteasome-mediated degradation, resulting in nuclear translocation of NF-κB that regulates the expression of hundreds of target genes by binding to the consensus sequence located in the promoter. Importantly, the expression of NF-κB p65 is enhanced in neurons, NFTs, and dystrophic neurites in the hippocampus and entorhinal cortex of AD brains [50]. A NF-κB-inducible microRNA, MiR-146a, reduces the expression of complement factor H (CFH), a negative regulator of proinflammatory responses in AD brains [51].

We also identified gene expression regulated by vitamin D receptor (VDR) as the third significant pathway in the molecular network of AGDs (Supplementary Fig. 2 online). Vitamin D plays a neuroprotective role by modulating neuronal calcium homeostasis. By forming a heterodimer with the retinoid X receptor (RXR), VDR activates the transcription of target genes with the vitamin D response element (VDRE) in the promoter. A significant association is found between VDR gene polymorphism and development of AD [52]. In AD brains, the expression of VDR and its target calbindin D28K is downregulated in hippocampal CA1 neurons [53].

In conclusion, KeyMolnet has effectively characterized molecular network of 2,883 ADGs and 559 IADGs. The common upstream search identified CREB as the principal transcription factor that regulates molecular networks of both ADGs and IADGs. Im-

munohistochemical study showed an abnormal accumulation of pCREB in GVD granules in hippocampal neurons of AD brains. These observations suggest that aberrant CREB-mediated gene regulation serves as a molecular biomarker of AD-related pathological processes, and support the hypothesis that sequestration of pCREB in GVD granules is in part responsible for deregulation of CREB-mediated gene expression in AD hippocampus.

5. Supplemental Material

Supplemental figures and tables can be found on http://www.my-pharm.ac.jp/~satoj/sub19.html as downloadable PDF files.

Acknowledegements

Human brain tissues were provided by Research Resource Network (RRN), Japan. This work was supported by a research grant to J-IS from the High-Tech Research Center Project, the Ministry of Education, Culture, Sports, Science and Technology (MEXT), Japan (S0801043), and from Research on Intractable Diseases, the Ministry of Health, Labour and Welfare of Japan.

References

[1] A. Serretti, P. Olgiati and D. De Ronchi, Genetics of Alzheimer's disease. A rapidly evolving field, *J Alzheimers Dis* **12** (2007), 73–92.

[2] S.F. Kingsmore, I.E. Lindquist, J. Mudge, D.D. Gessler and W.D. Beavis, Genome-wide association studies: progress and potential for drug discovery and development, *Nat Rev Drug Discov* **7** (2008), 221–230.

[3] S.D. Ginsberg, S.E. Hemby, V.M. Lee, J.H. Eberwine and J.Q. Trojanowski, Expression profile of transcripts in Alzheimer's disease tangle-bearing CA1 neurons, *Ann Neurol* **48** (2000), 77–87.

[4] V. Colangelo, J. Schurr, M.J. Ball, R.P. Pelaez, N.G. Bazan and W.J. Lukiw, Gene expression profiling of 12633 genes in Alzheimer hippocampal CA1: transcription and neurotrophic factor down-regulation and up-regulation of apoptotic and pro-inflammatory signaling, *J Neurosci Res* **70** (2002), 462–473.

[5] P. Katsel, C. Li and V. Haroutunian, Gene expression alterations in the sphingolipid metabolism pathways during progression of dementia and Alzheimer's disease: a shift toward ceramide accumulation at the earliest recognizable stages of Alzheimer's disease? *Neurochem Res* **32** (2007), 845–856.

[6] C. Williams, R. Mehrian Shai, Y. Wu, Y.H. Hsu, T. Sitzer, B. Spann, C. McCleary, Y. Mo and C.A. Miller, Transcriptome analysis of synaptoneurosomes identifies neuroplasticity genes overexpressed in incipient Alzheimer's disease, *PLoS ONE* **4** (2009), e4936.

[7] K. Oda, Y. Matsuoka, A. Funahashi and H. Kitano, A comprehensive pathway map of epidermal growth factor receptor signaling, *Mol Syst Biol* **1** (2005), 2005.0010.

[8] F. Noorbakhsh, C.M. Overall and C. Power, Deciphering complex mechanisms in neurodegenerative diseases: the advent of systems biology, *Trends Neurosci* **32** (2009), 88–100.

[9] R. Albert, H. Jeong and A.L. Barabasi, Error and attack tolerance of complex networks, *Nature* **406** (2000), 378–382.

[10] E.M. Blalock, J.W. Geddes, K.C. Chen, N.M. Porter, W.R. Markesbery and P.W. Landfield, Incipient Alzheimer's disease: microarray correlation analyses reveal major transcriptional and tumor suppressor responses, *Proc Natl Acad Sci USA* **101** (2004), 2173–2178.

[11] J.A. Miller, M.C. Oldham and D.H. Geschwind, A systems level analysis of transcriptional changes in Alzheimer's disease and normal aging, *J Neurosci* **28** (2008), 1410–1420.

[12] H. Sato, S. Ishida, K. Toda, R. Matsuda, Y. Hayashi, M. Shigetaka, M. Fukuda, Y. Wakamatsu and A. Itai, New approaches to mechanism analysis for drug discovery using DNA microarray data combined with KeyMolnet, *Curr Drug Discov Technol* **2** (2005) 89–98.

[13] D.W. Huang, B.T. Sherman and R.A. Lempicki, Systematic and integrative analysis of large gene lists using DAVID bioinformatics resources, *Nat Protoc* **4** (2009), 44–57.

[14] E.I. Boyle, S. Weng, J. Gollub, H. Jin, D. Botstein, J.M. Cherry and G. Sherlock, GO: TermFinder – open source software for accessing Gene Ontology information and finding significantly enriched Gene Ontology terms associated with a list of genes, *Bioinformatics* **20** (2004), 3710–3715.

[15] S.S. Mirra, A. Heyman, D. McKeel, S.M. Sumi, B.J. Crain, L.M. Brownlee, F.S. Vogel, J.P. Hughes, G. van Belle and L. Berg, The Consortium to Establish a Registry for Alzheimer's Disease (CERAD). Part II. Standardization of the neuropathologic assessment of Alzheimer's disease, *Neurology* **41** (1991), 479–486.

[16] H. Braak, I. Alafuzoff, T. Arzberger, H. Kretzschmar and K. Del Tredici, Staging of Alzheimer disease-associated neurofibrillary pathology using paraffin sections and immunocytochemistry, *Acta Neuropathol* **112** (2006), 389–404.

[17] T. Misawa, K. Arima, H. Mizusawa and J. Satoh, Close association of water channel AQP1 with amyloid-β deposition in Alzheimer disease brains, *Acta Neuropathol* **116** (2008), 247–260.

[18] B. Mayr and M. Montminy, Transcriptional regulation by the phosphorylation-dependent factor CREB, *Nat Rev Mol Cell Biol* **2** (2001), 599–609.

[19] B.E. Lonze and D.D. Ginty, Function and regulation of CREB family transcription factors in the nervous system, *Neuron* **35** (2002), 605–623.

[20] J. Satoh, Z. Illes, A. Peterfalvi, H. Tabunoki, C. Rozsa and T. Yamamura, Aberrant transcriptional regulatory network in T cells of multiple sclerosis, *Neurosci Lett* **422** (2007), 30–33.

[21] J. Satoh, T. Misawa, H. Tabunoki and T. Yamamura, Molecular network analysis of T-cell transcriptome suggests aberrant regulation of gene expression by NF-κB as a biomarker for relapse of multiple sclerosis, *Dis Markers* **25** (2008), 27–35.

[22] X. Zhang, D.T. Odom, S.H. Koo, M.D. Conkright, G. Canettieri, J. Best, H. Chen, R. Jenner, E. Herbolsheimer, E. Jacobsen, S. Kadam, J.R. Ecker, B. Emerson, J.B. Hogenesch, T. Unterman, R.A. Young and M. Montminy, Genome-wide analysis of cAMP-response element binding protein occupancy, phosphorylation, and target gene activation in human tissues, *Proc Natl Acad Sci USA* **102** (2005), 4459–4464.

[23] H. Viola, M. Furman, L.A. Izquierdo, M. Alonso, D.M. Barros, M.M. de Souza, I. Izquierdo and J.H. Medina, Phosphorylated cAMP response element-binding protein as a molecular marker of memory processing in rat hippocampus: effect of novelty, *J Neurosci* **20** (2000), RC112.

[24] M. Yamamoto-Sasaki, H. Ozawa, T. Saito, M. Rösler and P. Riederer, Impaired phosphorylation of cyclic AMP response element binding protein in the hippocampus of dementia of the Alzheimer type, *Brain Res* **824** (1999), 300–303.

[25] G.S. Griesbach, R.L. Sutton, D.A. Hovda, Z. Ying and F. Gomez-Pinilla, Controlled contusion injury alters molecular systems associated with cognitive performance, *J Neurosci Res* **87** (2009), 795–805.

[26] B. Gong, O.V. Vitolo, F. Trinchese, S. Liu, M. Shelanski and O. Arancio, Persistent improvement in synaptic and cognitive functions in an Alzheimer mouse model after rolipram treatment, *J Clin Invest* **114** (2004), 1624–1634.

[27] Z. Liang, F. Liu, I. Grundke-Iqbal, K. Iqbal and C.X. Gong, Down-regulation of cAMP-dependent protein kinase by over-activated calpain in Alzheimer disease brain, *J Neurochem* **103** (2007), 2462–2470.

[28] D.N. Arvanitis, A. Ducatenzeiler, J.N. Ou, E. Grodstein, S.D. Andrews, S.R. Tendulkar, A. Ribeiro-da-Silva, M. Szyf and A.C. Cuello, High intracellular concentrations of amyloid-β block nuclear translocation of phosphorylated CREB, *J Neurochem* **103** (2007), 216–228.

[29] O.V. Vitolo, A. Sant'Angelo, V. Costanzo, F. Battaglia, O. Arancio and M. Shelanski, Amyloid β-peptide inhibition of the PKA/CREB pathway and long-term potentiation: reversibility by drugs that enhance cAMP signaling, *Proc Natl Acad Sci USA* **99** (2002), 13217–13221.

[30] D. Puzzo, O. Vitolo, F. Trinchese, J.P. Jacob, A. Palmeri and O. Arancio, Amyloid-β peptide inhibits activation of the nitric oxide/cGMP/cAMP-responsive element-binding protein pathway during hippocampal synaptic plasticity, *J Neurosci* **25** (2005), 6887–6897.

[31] Q.L. Ma, M.E. Harris-White, O.J. Ubeda, M. Simmons, W. Beech, G.P. Lim, B. Teter, S.A. Frautschy and G.M. Cole, Evidence of Aβ- and transgene-dependent defects in ERK-CREB signaling in Alzheimer's models, *J Neurochem* **103** (2007), 1594–1607.

[32] Q. Li, H.F. Zhao, Z.F. Zhang, Z.G. Liu, X.R. Pei, J.B. Wang and Y. Li, Long-term green tea catechin administration prevents spatial learning and memory impairment in senescence-accelerated mouse prone-8 mice by decreasing $A\beta_{1-42}$ oligomers and upregulating synaptic plasticity-related proteins in the hippocampus, *Neuroscience* (2009), in press, doi:10.1016/j.neuroscience.2009.07.014.

[33] F.G. De Felice, A.P. Wasilewska-Sampaio, A.C. Barbosa, F.C. Gomes, W.L. Klein and S.T. Ferreira, Cyclic AMP enhancers and Aβ oligomerization blockers as potential therapeutic agents in Alzheimer's disease, *Curr Alzheimer Res* **4** (2007), 263–271.

[34] R.A. Nixon, Autophagy, amyloidogenesis and Alzheimer disease, *J Cell Sci* **120** (2007), 4081–4091.

[35] C.V. Garat, D. Fankell, P.F. Erickson, J.E. Reusch, N.N. Bauer, I.F. McMurtry and D.J. Klemm, Platelet-derived growth factor BB induces nuclear export and proteasomal degradation of CREB via phosphatidylinositol 3-kinase/Akt signaling in pulmonary artery smooth muscle cells, *Mol Cell Biol* **26** (2006), 4934–4948.

[36] S. Costes, B. Vandewalle, C. Tourrel-Cuzin, C. Broca, N. Linck, G. Bertrand, J. Kerr-Conte, B. Portha, F. Pattou, J. Bockaert and S. Dalle, Degradation of cAMP-responsive element-binding protein by the ubiquitin-proteasome pathway contributes to glucotoxicity in beta-cells and human pancreatic islets, *Diabetes* **58** (2009) 1105–1115.

[37] K. Okamoto, S. Hirai, T. Iizuka, T. Yanagisawa and M. Watanabe, Reexamination of granulovacuolar degeneration, *Acta Neuropathol* **82** (1991), 340–345.

[38] C. Stadelmann, T.L. Deckwerth, A. Srinivasan, C. Bancher, W. Brück, K. Jellinger and H. Lassmann, Activation of caspase-3 in single neurons and autophagic granules of granulovacuolar degeneration in Alzheimer's disease. Evidence for apoptotic cell death, *Am J Pathol* **155** (1999), 1459–1466.

[39] K. Leroy, A. Boutajangout, M. Authelet, J.R. Woodgett, B.H. Anderton and J.P. Brion, The active form of glycogen synthase kinase-3β is associated with granulovacuolar degeneration in neurons in Alzheimer's disease, *Acta Neuropathol* **103** (2002), 91–99.

[40] S. Lagalwar, R.W. Berry and L.I. Binder, Relation of hippocampal phospho-SAPK/JNK granules in Alzheimer's disease and tauopathies to granulovacuolar degeneration bodies, *Acta Neuropathol* **113** (2007), 63–73.

[41] A. Thakur, X. Wang, S.L. Siedlak, G. Perry, M.A. Smith and X. Zhu, c-Jun phosphorylation in Alzheimer disease, *J Neurosci Res* **85** (2007), 1668–1673.

[42] J.J. Hoozemans, E.S. van Haastert, D.A. Nijholt, A.J. Rozemuller, P. Eikelenboom and W. Scheper, The unfolded protein response is activated in pretangle neurons in Alzheimer's disease hippocampus, *Am J Pathol* **174** (2009), 1241–1251.

[43] A. Kadokura, T. Yamazaki, S. Kakuda, K. Makioka, C.A. Lemere, Y. Fujita, M. Takatama and K. Okamoto, Phosphorylation-dependent TDP-43 antibody detects intraneuronal dot-like structures showing morphological characters of granulovacuolar degeneration, *Neurosci Lett* (2009), in press, doi:10.1016/j.neulet.2009.06.024.

[44] D.W. Dickson, H. Ksiezak-Reding, P. Davies and S.H. Yen, A monoclonal antibody that recognizes a phosphorylated epitope in Alzheimer neurofibrillary tangles, neurofilaments and tau proteins immunostains granulovacuolar degeneration, *Acta Neuropathol* **73** (1987), 254–258.

[45] W. Bondareff, C.M. Wischik, M. Novak and M. Roth, Sequestration of tau by granulovacuolar degeneration in Alzheimer's disease, *Am J Pathol* **139** (1991), 641–647.

[46] B. Boland, A. Kumar, S. Lee, F.M. Platt, J. Wegiel, W.H. Yu and R.A. Nixon, Autophagy induction and autophagosome clearance in neurons: relationship to autophagic pathology in Alzheimer's disease, *J Neurosci* **28** (2008) 6926–6937.

[47] W.Y. Ong, H.M. Lim, T.M. Lim and B. Lutz, Kainate-induced neuronal injury leads to persistent phosphorylation of cAMP response element-binding protein in glial and endothelial cells in the hippocampus, *Exp Brain Res* **131** (2000), 178–186.

[48] L.J. Cox, U. Hengst, N.G. Gurskaya, K.A. Lukyanov and S.R. Jaffrey, Intra-axonal translation and retrograde trafficking of CREB promotes neuronal survival, *Nat Cell Biol* **10** (2008) 149–159.

[49] I Granic, A.M. Dolga, I.M. Nijholt, G. van Dijk and U.L. Eisel, Inflammation and NF-κB in Alzheimer's disease and diabetes, *J Alzheimers Dis* **16** (2009), 809–821.

[50] K. Terai, A. Matsuo and P.L. McGeer, Enhancement of immunoreactivity for NF-κB in the hippocampal formation and cerebral cortex of Alzheimer's disease, *Brain Res* **735** (1996), 159–168.

[51] W.J. Lukiw, Y. Zhao and J.G. Cui, An NF-κB-sensitive micro RNA-146a-mediated inflammatory circuit in Alzheimer

disease and in stressed human brain cells, *J Biol Chem* **283** (2008), 31315–31322.

[52] D. Gezen-Ak, E. Dursun, T. Ertan, H. Hanağasi, H. Gürvit, M. Emre, E. Eker, M. Oztürk, F. Engin and S. Yilmazer, Association between vitamin D receptor gene polymorphism and Alzheimer's disease, *Tohoku J Exp Med* **212** (2007), 275–282.

[53] M.K. Sutherland, M.J. Somerville, L.K. Yoong, C. Bergeron, M.R. Haussler and D.R. McLachlan, Reduction of vitamin D hormone receptor mRNA levels in Alzheimer as compared to Huntington hippocampus: correlation with calbindin-28k mRNA levels, *Brain Res Mol Brain Res* **13** (1992), 239–250.

Cell Mol Neurobiol (2009) 29:423–438
DOI 10.1007/s10571-008-9338-2

ORIGINAL PAPER

Gene Expression Profiling of Human Neural Progenitor Cells Following the Serum-Induced Astrocyte Differentiation

Shinya Obayashi · Hiroko Tabunoki · Seung U. Kim · Jun-ichi Satoh

Received: 16 August 2008 / Accepted: 10 December 2008 / Published online: 7 January 2009
© Springer Science+Business Media, LLC 2008

Abstract Neural stem cells (NSC) with self-renewal and multipotent properties could provide an ideal cell source for transplantation to treat spinal cord injury, stroke, and neurodegenerative diseases. However, the majority of transplanted NSC and neural progenitor cells (NPC) differentiate into astrocytes in vivo under pathological environments in the central nervous system, which potentially cause reactive gliosis. Because the serum is a potent inducer of astrocyte differentiation of rodent NPC in culture, we studied the effect of the serum on gene expression profile of cultured human NPC to identify the gene signature of astrocyte differentiation of human NPC. Human NPC spheres maintained in the serum-free culture medium were exposed to 10% fetal bovine serum (FBS) for 72 h, and processed for analyzing on a Whole Human Genome Microarray of 41,000 genes, and the microarray data were validated by real-time RT-PCR. The serum elevated the levels of expression of 45 genes, including ID1, ID2, ID3, CTGF, TGFA, METRN, GFAP, CRYAB and CSPG3, whereas it reduced the expression of 23 genes, such as DLL1, DLL3, PDGFRA, SOX4, CSPG4, GAS1 and HES5. Thus, the serum-induced astrocyte differentiation of human NPC is characterized by a counteraction of ID family genes on Delta family genes. Coimmunoprecipitation analysis identified ID1 as a direct binding partner of a proneural basic helix-loop-helix (bHLH) transcription factor MASH1. Luciferase assay indicated that activation of the DLL1 promoter by MASH1 was counteracted by ID1. Bone morphogenetic protein 4 (BMP4) elevated the levels of ID1 and GFAP expression in NPC under the serum-free culture conditions. Because the serum contains BMP4, these results suggest that the serum factor(s), most probably BMP4, induces astrocyte differentiation by upregulating the expression of ID family genes that repress the proneural bHLH protein-mediated Delta expression in human NPC.

Keywords Astrocytes · Delta family genes · Human neuronal progenitor cells · ID family genes · Microarray

Abbreviations

NSC	Neural stem cells
NPC	Neural progenitor cells
CNS	Central nervous system
BBB	Blood–brain barrier
bHLH	Basic helix-loop-helix
FBS	Fetal bovine serum
EGF	Epidermal growth factor
bFGF	Basic fibroblast growth factor
LIF	Leukemia inhibitory factor
TGF	Transforming growth factor
RT-PCR	Reverse transcription-polymerase chain reaction
DAVID	Database for annotation visualization and integrated discovery
GO	Gene Ontology
GFAP	Glial fibrillary acidic protein
BMP4	Bone morphogenetic protein 4

S. Obayashi · H. Tabunoki · J.-i. Satoh (✉)
Department of Bioinformatics and Molecular Neuropathology, Meiji Pharmaceutical University, 2-522-1 Noshio, Kiyose, Tokyo 204-8588, Japan
e-mail: satoj@my-pharm.ac.jp

S. U. Kim
Division of Neurology, Department of Medicine, University of British Columbia Hospital, University of British Columbia, Vancouver, BC, Canada

Introduction

Neural stem cells (NSC) with self-renewal and multipotent properties are distributed broadly in the niche of germinal zones in the embryonic and adult mammalian central nervous system (CNS). NSC, unlimitedly propagated in vitro and genetically manipulated ex vivo, could provide an ideal cell source for transplantation to compensate for cell damage in spinal cord injury, stroke, and neurodegenerative diseases (Martino and Pluchino 2006). However, the majority of transplanted NSC and neural progenitor cells (NPC), the cells committed to differentiation into the neuronal lineage, differentiate into astrocytes in vivo under pathological environments in the CNS, which contribute to glial scar formation that inhibits axonal regeneration (Pallini et al. 2005; Ishii et al. 2006). Oxidative stress mediators abundant in pathological lesions elevate the expression of histone deacethylase (HDAC) Sirt1 in mouse NPC, which cooperates with an inhibitory basic helix-loop-helix (bHLH) protein HES1 to mediate epigenetic silencing of a proneural bHLH transcription factor MASH1, leading to astrocyte differentiation of NPC (Prozorovski et al. 2008). To obtain a subset of neurons desirable for cell replacement therapy for human neurological diseases, we should intensively clarify the complex interaction of intrinsic genetic programs and environmental factors that regulate human NSC and NPC proliferation and differentiation. However, at present, molecular mechanisms underlying astrocytic differentiation of human NSC and NPC in vitro and in vivo remain largely unknown.

DNA microarray technology is a powerful approach that allows us to systematically monitor gene expression profile of neural cells during differentiation under development. Microarray analysis showed that neuronal differentiation of human NSC in culture involves the regulation of hundreds of genes, including those essential for Wnt and TGF-beta signaling pathways (Cai et al. 2006). By comparing gene expression profiles between human NPC and differentiated neurons, a previous study identified both PDGF receptor alpha (PDGFRA) and IGF-binding protein 4 (IGFBP4) as key proneural differentiation factors (Yu et al. 2006). A recent study discovered 38 genes expressed commonly between adult and fetal human NPC (Maisel et al. 2007). Recently, we have characterized the DNA damage-responsive gene signature of human astrocytes in culture (Satoh et al. 2006).

Because the serum is a potent inducer of astrocyte differentiation of rodent NSC and NPC in culture (Chiang et al. 1996; Brunet et al. 2004), and the serum components enter the CNS via the disrupted blood–brain barrier (BBB) at the site of CNS injury and ischemia, we studied the effect of the serum on gene expression profile of human NPC in culture by analyzing with a whole genome-scale microarray to identify the gene signature of astrocyte differentiation of human NPC.

Methods

Neural Progenitor Cells in Culture

Cryopreserved human NPC, isolated from the brain of an 18.5-week-old female Caucasian under informed consent, were obtained from Cambrex (Walkersville, MD, USA) as a commercially available product (CC-2599). NPC were plated in a 6-well culture plate coated with polyethyleneimine, and incubated at 37°C in a 5% CO_2/95% air incubator in the NPC medium, composed of the serum-free DMEM/F-12 medium (Invitrogen, Carlsbad, CA, USA) supplemented with a mixture of insulin–transferrin–selenium (ITS) (Invitrogen), 20 ng/ml recombinant human EGF (Higeta, Tokyo, Japan), 20 ng/ml recombinant human bFGF (PeproTech EC, London, UK), and 10 ng/ml recombinant human LIF (Chemicon, Temecula, CA, USA), according to the methods described previously (Carpenter et al. 1999). The half of the medium was renewed every 4 days. Following incubation for several months, NPC in culture continued to proliferate by forming free floating or loosely attached growing spheres. For microarray analysis, nonpassage NPC spheres were harvested, replated in a non-coated 6-well culture plate, and incubated further for 72 h in the NPC medium with or without inclusion of 10% fetal bovine serum (FBS) (Biowest, Miami, FL, USA). In some experiments, NPC were incubated for 72 h in the NPC medium with or without inclusion of 50 ng/ml recombinant human BMP4 (PeproTech).

Human cell lines, such as NTera2 teratocarcinoma, Y79 retinoblastoma, SK-N-SH neuroblastoma, IMR-32 neuroblastoma, U-373MG astrocytoma, HMO6 microglia, HeLa cervical carcinoma, and HepG2 hepatoblastoma, were maintained as described previously (Satoh et al. 2007).

Gene Expression Profiling

Five micrograms of total RNA was isolated from NPC cells by using TRIZOL reagent (Invitrogen). It was in vitro amplified once, and cRNA was processed for microarray analysis on a Whole Human Genome Oligonucleotide Microarray (G4112A, 41,000 genes; Agilent Technologies, Palo Alto, CA, USA), as described previously (Satoh et al. 2006). cRNA prepared from NPC spheres without exposure to the serum (S−) was labeled with a fluorescent dye Cy3, while cRNA of NPC spheres with exposure to the serum (S+) was labeled with Cy5. The array was hybridized at

60°C for 17 h in the hybridization buffer containing equal amounts of Cy3- or Cy5-labeled cRNA. Then, it was scanned by the Agilent scanner (Agilent Technologies). The data were analyzed by using the Feature Extraction software (Agilent Technologies). The fluorescence intensities (FI) of individual spots were quantified following global normalization between Cy3 and Cy5 signals and subsequent Lowess normalization. The ratio of FI of Cy5 signal versus FI of Cy3 signal exceeding 2.0 was defined as significant upregulation, whereas the ratio smaller than 0.5 was considered as substantial downregulation.

Real-Time RT-PCR Analysis

DNase-treated total cellular RNA was processed for cDNA synthesis using oligo(dT)$_{12-18}$ primers and SuperScript II reverse transcriptase (Invitrogen). Then, cDNA was amplified by PCR in LightCycler ST300 (Roche Diagnostics, Tokyo, Japan) using SYBR Green I and primer sets listed in Table 1. The expression levels of target genes were standardized against those of the glyceraldehyde-3-phosphate dehydrogenase (G3PDH) gene detected in parallel in identical cDNA samples. All the assays were performed in triplicate.

Functional Annotation and Molecular Network Analysis

Functional annotation of significant genes identified by microarray analysis was searched by the web-accessible program named Database for Annotation, Visualization and Integrated Discovery (DAVID) version 2008, National Institute of Allergy and Infectious Diseases (NIAID), National Institutes of Health (NIH) (david.abcc.ncifcrf.gov) (Dennis et al. 2003). DAVID covers more than 40 annotation categories, including Gene Ontology (GO) terms, protein–protein interactions, protein functional domains, disease associations, biological pathways, sequence general features, homologies, gene functional summaries, and tissue expressions. By importing the list of the National Center for Biotechnology Information (NCBI) Entrez Gene IDs, this program creates the functional annotation chart, an annotation-term-focused view that lists annotation terms and their associated genes under study. To avoid excessive count of duplicated genes, the Fisher's exact test is calculated based on corresponding DAVID gene IDs by which all redundancies in original IDs are removed.

KeyMolnet is a knowledge-based content database that focuses on relationships among human genes, molecules, diseases, pathways and drugs, which were manually curated by expert biologists (www.immd.co.jp/en/keymolnet/index.html) (Sato et al. 2005). They are categorized into the core contents collected from selected review articles with the highest reliability or the secondary contents extracted from abstracts of PubMed database. The "N-points to N-points" network-search algorithm identifies the molecular network constructed by the shortest route connecting the start point molecules and the end point molecules. The generated network was compared side by side with 346 human canonical pathways of the KeyMolnet library. The algorithm counting the number of overlapping molecular relations between the extracted network and the canonical pathway makes it possible to identify the canonical pathway showing the statistically significant contribution to the extracted network.

Immunohistochemistry

For immunocytochemistry, NPC attached on poly-L-lysine-coated cover glasses were fixed with 4% PFA in 0.1 M phosphate buffer, pH 7.4 at room temperature (RT) for 5 min, followed by incubation with phosphate-buffered saline (PBS) containing 0.5% Triton X-100 at RT for 3 min. After blocking non-specific staining by PBS containing 10% NGS, the cells were incubated at RT for 30 min with a mixture of mouse monoclonal anti-GFAP antibody (GA5; Nichirei, Tokyo, Japan) and rabbit polyclonal anti-nestin antibody (AB5922; Chemicon) or rabbit polyclonal anti-ID1 antibody (C-20; Santa Cruz Biotechnology, Santa Cruz, CA, USA). Then, they were incubated at RT for 30 min with a mixture of Alexa Fluor 488-conjugated anti-rabbit IgG (Invitrogen) and Alexa Fluor 568-conjugated anti-mouse IgG (Invitrogen). After several washes, they were examined on the Olympus BX51 universal microscope.

Western Blot Analysis

To prepare total protein extract, the cells were homogenized in RIPA buffer containing and a cocktail of protease inhibitors (Sigma, St. Louis, MO, USA). Following centrifugation at 12,000 rpm for 10 min at RT, the supernatant was collected and separated on a 12% or 15% SDS–PAGE gel. After gel electrophoresis, the protein was transferred onto nitrocellulose membranes, and the blots were labeled at RT overnight with anti-GFAP antibody (GA5) or anti-ID1 antibody (C-20). Then, they were incubated at RT for 30 min with HRP-conjugated anti-mouse or rabbit IgG (Santa Cruz Biotechnology). The specific reaction was visualized by exposing to a chemiluminescence substrate (Pierce, Rockford, IL, USA). After the antibodies were stripped by incubating the membranes at 50°C for 30 min in stripping buffer, composed of 62.5 mM Tris-HCl, pH 6.7, 2% SDS and 100 mM 2-mercaptoethanol, the blots were processed for relabeling with anti-HSP60 antibody (N-20; Santa Cruz Biotechnology).